

Crack Opening Behavior of Concrete Reinforced with High Strength Reinforcing Steel

Amir Soltani^{1)*}, Kent A. Harries²⁾, and Bahram M. Shahrooz³⁾

(Received January 29, 2013, Accepted August 16, 2013)

Abstract: A major difference between high-strength reinforcing steel and conventional steel in concrete is that the service-load steel stress is expected to be greater. Consequently, the service-load steel strains are greater affecting cracking behavior. A parametric study investigating crack widths and patterns in reinforced concrete prisms is presented in order to establish limits to the service-load steel stress and strain. Additionally, based on the results of available flexural tests, crack widths at service load levels were evaluated and found to be within presently accepted limits for highway bridge structures, and were predictable using current AASHTO provisions. A limitation on service-level stresses of $f_s \leq 414$ MPa (60 ksi) is nonetheless recommended.

Keywords: crack opening, crack width, bond characteristics, high-strength reinforcing steel.

1. Introduction

Reinforced concrete members are typically designed based on strength at ultimate limit state and subsequently checked for deflection and crack control at serviceability limit state. Although the service checks are generally conservative—based on limiting stresses in the structure at service loads—the adoption of higher strength materials suggests potential problems under service conditions. The material strength of steel reinforcement and concrete, bond characteristics, size of a member, and amount of reinforcement are all factors affecting the development of cracks in reinforced concrete members. Concrete members reinforced with high strength steel reinforcement [having a yield strength, f_y , greater than 690 MPa (100 ksi)] have different behavior due to the expected higher service loads, compared to concrete members reinforced with conventional steel bars [$f_y = 414$ MPa (60 ksi)]. Using a higher strength reinforcing steel could provide various benefits to the concrete construction industry by reducing member cross sections and reinforcement quantities, which would lead to savings in materials, shipping, and placement costs. Reducing reinforcement quantities may also reduce congestion problems leading to better quality of construction. Finally, coupling high-strength steel

reinforcement with high-performance concrete should result in a more efficient use of both materials. This approach, however, affects the flexural stiffness, as measured by the effective moment of inertia, I_e , of a cracked reinforced concrete member and results in different deflection and cracking behaviors.

1.1 High Strength Reinforcing Steel

The design of reinforced concrete structures in the United States is dominated by the use of steel reinforcement with yield strength, f_y , equal to 414 MPa (60 ksi). Design with steel having higher yield strength values is permitted although the yield strength used in strength calculations is limited. Currently, ACI 318 (2011) permits design using steel reinforcement with yield strength not exceeding 552 MPa (80 ksi). The *AASHTO LRFD Bridge Design Specifications* (AASHTO 2010) similarly limit the use of reinforcing steel yield strength in design to no less than 414 MPa (60 ksi) and no greater than 517 MPa (75 ksi), although exceptions are permitted with owner's approval. Both ACI and AASHTO limits have been written and interpreted to not exclude the use of higher strength grades of steel, but only to limit the value of yield strength that may be used in design, thus, reducing the efficiency of using these materials.

The limits on yield strength are required to ensure adequate ductility of a section and are related to the prescribed limit on concrete compressive strain of 0.003. The limits on yield strength also serve to control of crack widths at service loads. Crack width is a function of steel strain and consequently steel stress (Nawy 1968). Therefore, the stress in the steel reinforcement will always need to be limited to some extent in order to prevent cracking from affecting

¹⁾Department of Mechanical and Civil Engineering, Purdue University Calumet, Hammond, IN 46323, USA.

*Corresponding Author; E-mail: amirsolt@yahoo.com

²⁾Department of Civil and Environmental Engineering, University of Pittsburgh, Pittsburgh, PA 15213, USA.

³⁾School of Advanced Structures, University of Cincinnati, Cincinnati, OH 45267, USA.

serviceability of the structure. However, with recent improvements to the properties of concrete, the ACI 318 limit of 552 MPa (80 ksi) and AASHTO limit of 517 MPa (75 ksi) on the steel reinforcement yield strength are believed to be unnecessarily conservative for new designs. Additionally, an argument can be made that if a higher strength reinforcing steel is used but not fully taken into account in design, there may be an inherent overstrength in the member that has not been properly incorporated in design.

Steel reinforcement with yield strength exceeding 552 MPa (80 ksi) is commercially available and being used in the United States. ASTM A1035 (2009) is specified to exceed 690 MPa (100 ksi) or 827 MPa (120 ksi).

2. Crack Formation and Crack Control

Crack formation refers to the incidence of any narrow, irregular opening of indefinite dimensions resulting from shrinkage, flexural or direct tension stresses, or internal expansion resulting from the products of corrosion or deleterious aggregates. The incidence of flexural and direct tension cracking that occurs at various stages is defined in relation to the stresses in the reinforcement at the cracked section (Reis et al. 1964). Since steel has a constant Young's modulus (at service load levels) regardless of grade, this approach is possibly better described with respect to steel strain, rather than stress. The following brief description of load-induced cracking in a tension zone is based on that reported by Reis et al.

The first stage of cracking is concerned with those cracks produced by shrinkage, corrosive effects, and low flexural loads in which the measured steel strain is well below $\epsilon_s = 0.0005$ [$f_s \approx 100$ MPa (14 ksi)]. Cracks of this type are referred to as primary cracks. The second stage of cracking is concerned with those cracks that result from the difference in inextensibility between the concrete and steel, and the bonding forces that exist between the two. Cracks formed by this mechanism are referred to as secondary cracks. Secondary crack formation is usually studied by examining the portion of the beam between two adjacent primary cracks or by analyzing the model of an axially loaded reinforced concrete prism in tension (as is done in this study). The steel strains during the second stage of cracking are usually greater than 0.0005. There is considerable disagreement among the theories of secondary cracking concerning the significance of the variables involved, especially the nature of the bond stress distribution along the reinforcement between adjacent primary cracks. The third stage of cracking, also referred to as the equilibrium stage, occurs when no further secondary cracks can be formed, and existing cracks continue to widen. The steel strain is usually greater than 0.001 [$f_s \approx 200$ MPa (30 ksi)] at this stage of cracking. Although the initiation of primary cracks is important, the main concern of this research is with the distribution of second and third stage cracks, which occur at higher steel stresses.

When a reinforced concrete member is loaded gradually in pure tension, cracking of the concrete will take place in one or more places along the length of the member when the tensile stress in the concrete exceeds the tensile strength of the concrete. After cracking, the tensile stress in the concrete adjacent to the crack is relieved because of the slip that takes place between the concrete and reinforcement at this location. Away from the crack, tensile stress in the concrete between cracks is present because of the bond between the reinforcement and concrete. The distribution and magnitude of the bond stress along the reinforcement will determine the distribution of the concrete stress between cracks along the length of the member. As tension loading is increased, cracking will continue to take place until the stress in the concrete between cracks no longer exceeds the concrete tensile strength. This stage occurs due to excessive slip and the reduction of distance between cracks. Essentially, the distance between cracks becomes sufficiently small that the stress to cause concrete cracking can no longer be developed by the reinforcing steel present. When this condition is reached, the crack spacing reaches its minimum, but the crack widths will continue to increase as the tensile stress in the reinforcement increases (i.e., third stage cracking as described by Reis et al. 1964). Assuming this behavior to be valid and that second stage cracking is fully developed by $\epsilon_s = 0.001$ (Reis et al. 1964), it may be hypothesized that crack patterns in members having high strength reinforcing steel will not vary from those having conventional steel. Thus, only crack width, and not crack spacing, will be affected by utilizing the higher strength steel. The cracking behavior of reinforced concrete members in axial tension is similar to that of flexural members, except that the maximum crack width is larger than that predicted by the expressions for flexural members (Broms 1965a, b). The lack of strain gradient and restraint imposed by the compression zone of flexural members is probably the reason for the lower flexural crack width.

The final crack pattern in a member is determined at the end of the second stage of cracking (Reis et al. 1964). Therefore, controlling the spacing and width of secondary cracks are most important to the overall performance of a member. Based on the early studies reported above, the following are the main factors involved in the control of the final crack pattern: (a) reinforcement stress, (b) the bond characteristics of reinforcement, (c) the distribution of reinforcement over the effective concrete area subject to tension, (d) the diameter of reinforcement, (e) the percentage of reinforcement, (f) the concrete cover over the reinforcement, and (g) the material properties of the concrete.

Based on the physical model, Frosch (1999, 2001) developed the following simple equation to predict crack widths, w_c :

$$w_c = 2 \frac{f_s}{E_s} \beta \sqrt{d_c^2 + (s/2)^2} \quad (1)$$

where f_s is the stress in reinforcing steel, E_s the Young's modulus of reinforcing steel, $\beta = 1 + 0.08d_c$, d_c the

distance from tension face to centroid of nearest reinforcing bar, s is the spacing of longitudinal reinforcing bars.

ACI Committee 318 (2011) made some modifications to this equation and adopted a new crack control approach to evaluate the maximum longitudinal bar spacing, s , for the 1999 code as follows:

$$s \leq 380 \left(\frac{280}{f_s} \right) - 2.5c_c \leq 300 \left(\frac{280}{f_s} \right) \quad (\text{MPa and mm})$$

$$s \leq \frac{540}{f_s} - 2.5c_c \leq \frac{432}{f_s} \quad (\text{ksi and in.}) \quad (2)$$

where c_c is the clear concrete cover for reinforcement nearest the tension face

Since the recalibration of ACI 318 load factors in 2002, Eq. 2 is calibrated for a de facto assumed crack width of $w_c = 0.46 \text{ mm}$ (0.018 in.).

Similar requirements in AASHTO (2010) take a similar form as the ACI equation:

$$s \leq \frac{138000\lambda_d}{\beta f_s} - 2d_c \quad (\text{MPa and mm})$$

$$s \leq \frac{700\lambda_d}{\beta f_s} - 2d_c \quad (\text{psi and in.}) \quad (3)$$

For Class 1 exposure (moderate exposure), the equation is calibrated, through $\gamma_d = 1$, for a crack width of 0.43 mm (0.017 in.); for Class 2 exposure (severe exposure), $\gamma_d = 0.75$. The de facto crack width (γ_d) is 0.43 mm.

In members having high-strength reinforcing bars, early studies showed that an increase in crack width is due to an increase in steel stress and, to a lesser extent, due to an increase in the curvature of the member. Thomas (1936) pointed out that an increase in the curvature at a constant steel stress tends to distribute the cracking rather than widening individual cracks. An increase in the steel stress affects the difference in the elongation between the reinforcing steel and concrete and causes additional slip to occur. This slip is the main cause of the increase in crack size. Slip occurs in the vicinity of a crack and extends to a point where the differential strain is zero. At that point the bond stress and resistance to slip reach maximum values and decrease toward the mid-point between cracks. The overall values of bond force decrease with an increase in load. This decrease is attributed to (a) the effects of the increase in transverse contraction of the reinforcing bar (i.e., Poisson effect) and (b) the deterioration of the concrete at the concrete-steel interface (Odman 1962). Therefore, the crack width increases while the crack spacing remains constant. If the load is increased further, the slip between concrete and reinforcement continues to increase. Due to the comparatively low values of concrete extensibility, the increase in crack width can be considered essentially equal to the accumulation of the slip between adjacent cracks.

3. Research Significance

The adopted equations for calculation of crack width and crack spacing are based on the use of conventional steel. However, concrete members reinforced with high strength steel reinforcement [having a yield strength, f_y , greater than 690 MPa (100 ksi)] have different behavior due to the expected higher service loads. An empirical parametric procedure has been introduced for determination of crack opening (crack width and crack spacing) in a reinforced concrete prism. Effective parameters have been investigated and finally the result has been compared to the available experimental data.

4. Parametric Study of Crack Characterization

In the case of using conventional steel bars in flexural members, it has been shown that during the second stage of cracking, when steel strains are usually greater than 0.0005, the presence of existing primary cracks affects the formation of secondary cracks under increasing moment. Away from a primary crack, stresses are transferred by bond from the reinforcement to the concrete. If enough force is transferred from the steel at the crack to the concrete away from the crack, the strains that are developed may exceed the strain capacity or the tensile strength of the concrete at a section and another crack will form perpendicular to the reinforcement. Theoretically, the section at which secondary crack formation occurs is midway between existing cracks. This mechanism continues until the tensile forces developed through bond transfer are insufficient to produce additional cracks. To compare and demonstrate the crack behavior of members reinforced with conventional steel bars and members reinforced with high-strength steel bars, a relatively complex material modeling in a simple direct tension model is used.

In general, the absolute displacements of the steel u_s , and of the concrete u_c between adjacent cracks in a concrete member are different. Due to this relative displacement (often referred to as 'slip'), $s = u_s - u_c$, bond stresses (technically, interfacial shear stresses) are generated between the concrete and the reinforcing steel. The magnitude of these bond stresses depends on the surface condition and deformation pattern (ribs) of the reinforcing steel, the concrete strength, f_c , concrete quality, and the degree of slip itself. Between adjacent cracks, a part of the tension force in the reinforcing steel acting at the crack is transferred into the concrete by bond. This transfer takes place over a length of bar referred to as the 'transmission length', L_t . This mechanism is associated with the so-called "tension stiffening" effect. Bischoff and Paixao (2004) and Bischoff (2005, 2007) used the concept of tension stiffening to determine the effective moment of inertia of concrete sections. They modeled the concrete contribution to

reinforced beam behavior with a tension stiffening factor that decreases with increasing load once the member has cracked. Finite element analysis of reinforced concrete beams under monotonic loads (Kwak and Filippou 1990) showed that the tension stiffening and bond-slip have opposing effects and can cancel each other in the response of lightly reinforced concrete beams. More extensive analytical study on tension stiffening in concrete beams shows that tension stiffening in axial members is not quite the same as that in flexural members due to the curvature (Ng et al. 2010). The decrease of the relative displacement along the transmission length, L_I , is characterized by the difference between the steel (ϵ_s) and concrete (ϵ_c) strains (CEB-FIP 1990):

$$\frac{ds}{dx} = \epsilon_s - \epsilon_c \quad (4)$$

As shown in the Fig. 1, in a reinforced concrete member subjected to tension, T (or the tension zone in a flexural member), the reinforcement at both loaded ends (which may be interpreted as crack locations) sustains the total external force with the stress f_{s0} . At an arbitrary location between cracks, however, the tensile stress in the reinforcement is smaller than f_{s0} ; this difference is transferred to the concrete by bond along the transmission length, L_I . From force equilibrium, therefore, the following relationship is valid at an arbitrary section located at distance, x .

$$T = A_s f_{s0} = T_s + T_c = A_s f_s(x) + A_c f_c(x) \quad (5)$$

where A_s is the area of reinforcing steel, A_c the area of concrete, $f_c(x)$ the stress in concrete at x , $f_s(x)$ is the stress in steel at location x

If one assumes the stress and strain in both reinforcement and concrete to have a linear relationship and concrete has not developed any cracks then Eq. (5) can be rewritten as follows:

$$T = A_s f_{s0} = A_s E_s \epsilon_s(x) + A_c E_c \epsilon_c(x) \quad 0 \leq x \leq L/2 \quad (6)$$

where E_c is the tensile modulus of elasticity of concrete.

If the length L is adequate to develop the full bond stress, at a distance L_I the reinforcement and concrete have the same strain ($\epsilon_s = \epsilon_c = \epsilon_2$); that is, there is a region experiencing no relative displacement (slip) between the concrete and steel (Fig. 1a). In this 'no slip' region, the applied tension force is distributed in proportion to the stiffness of the effective concrete and reinforcement and the bond stress is equal to zero. The total applied load in the no slip region is:

$$T = f_{s0} A_s = (E_c A_c + E_s A_s) \epsilon_2(x) \quad L_I \leq x \leq L/2 \quad (7)$$

To obtain the value of L_I and ϵ_2 , an additional relationship is required. Considering equilibrium on either side of a crack, as shown in Fig. 2, requires:

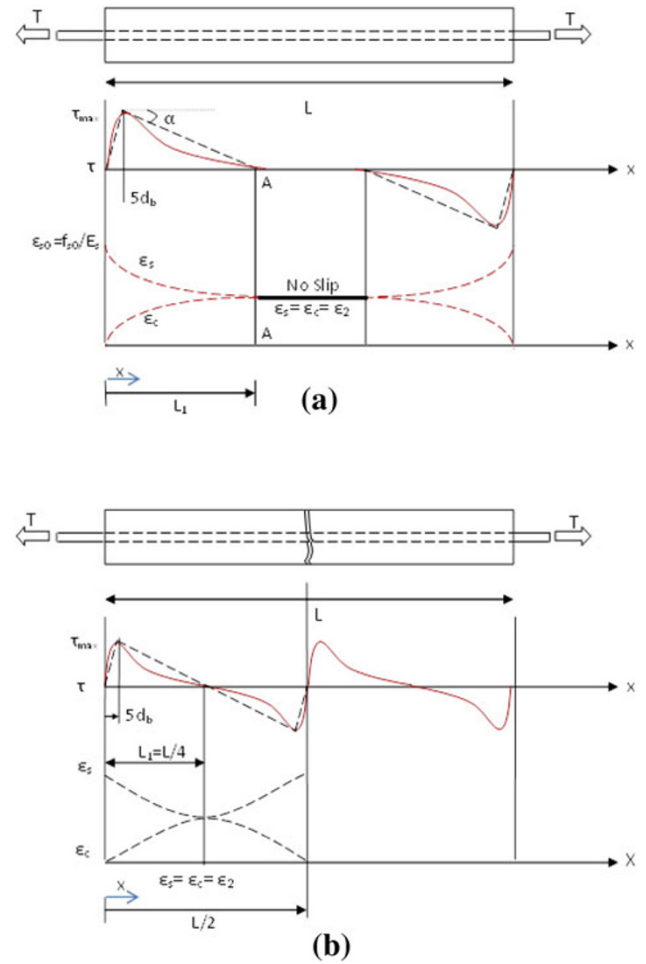


Fig. 1 Crack development in direct tension test. **a** Bond stress and resulting steel and concrete strain distribution before cracking. **b** No additional cracks have been developed after the first series of cracks at the tension load (T_1).

$$T(x) = T - \int_0^x \tau(x) p dx \quad (8)$$

where $\tau(x)$ is the force in the bar at x , $\tau(x)$ the bond stress distribution along the length of the bar and p is the bar circumference, assumed constant along the bar length.

Therefore, at L_I :

$$T(L_I) = \epsilon_2 E_s A_s = f_{s0} A_s - \int_0^{L_I} \tau(x) p dx \quad (9)$$

The relative bond stress relationship along the length of the bar is also required. The derived mechanics-based relationships show that bond stress is a function of relative bar slip; slip is a function of bar force, and bar force is a function of bond stress. As a result, even relatively simple bond stress-slip models require an iterative solution that must be evaluated using approximate methods. To simplify this process, a simple triangular form for the bond stress distribution along the length L_I is assumed (Fig. 1, dashed

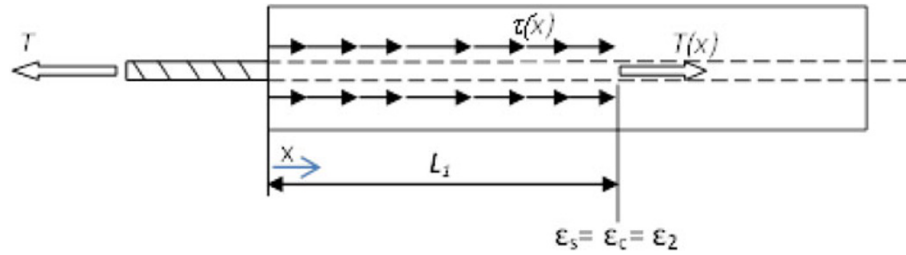


Fig. 2 Free body diagram of reinforcing steel in segment to one side of crack.

lines). This form requires two assumptions: firstly, a value for the maximum bond stress; in this study, the CEB-FIP (1990) value for good bond conditions, $\tau_{\max} = 0.17\sqrt{f'_c}$ (MPa) = $2\sqrt{f'_c}$ (psi) is adopted. Secondly, the distance over which τ_{\max} is developed is required; in this study, the CEB-FIP recommendation of 5 bar diameters ($5d_b$) is adopted as shown in Fig. 1. The formation of bond stress along the length of a bar changes as the tension force increases. Figure 3 illustrates the development of bond stress along the length of the bar. Based on these simplifications, values of L_1 and ε_2 can be found by solving Eqs. (7) and (9).

In order to determine the crack development in a member, the total force transmitted from the reinforcement to the concrete is calculated:

$$T_c = f_c A_c = E_c \varepsilon_2 A_c = \int_0^{L_1} p \tau(x) dx \quad (10)$$

If L_1 is sufficiently long to transfer a cumulative tensile stress resulting in a concrete stress, f_c , greater than ultimate tension capacity of concrete f_{cr} , then cracks will form. At the same stress level, additional cracks will continue to develop until the distance between adjacent cracks is no longer adequate to transfer sufficient tension to develop a new crack.

While the tension load (T) increases beyond that causing the first series of cracks, the relative strain in the reinforcement at the loaded ends, and cracks will increase. According to Fig. 3, the arbitrary location where strain in the reinforcement is equal to the strain in the concrete (Point B) occurs at a distance $L_2 > L_1$. In this case, the bond stress distribution along the length of the reinforcement corresponding to the tension force will be in a new form in which the angle of the descending branch, α , decreases (in Fig. 3, $\alpha_2 < \alpha_1$). The cumulative bond stress increases while α decreases. As a result, more force is transferred to the concrete section; and the additional force may or may not cause more cracks between the first cracks. The process continues until the transferred tension stress in the concrete section no longer exceeds f_{cr} .

4.1 Crack Behavior for a Concrete Prism Reinforced with a High-Strength Steel Bar

To investigate the effect of using higher-strength reinforcing steel on cracking behavior, the approach described above is adopted in a parametric study shown schematically in Fig. 4. The study considers a single bar is subject to

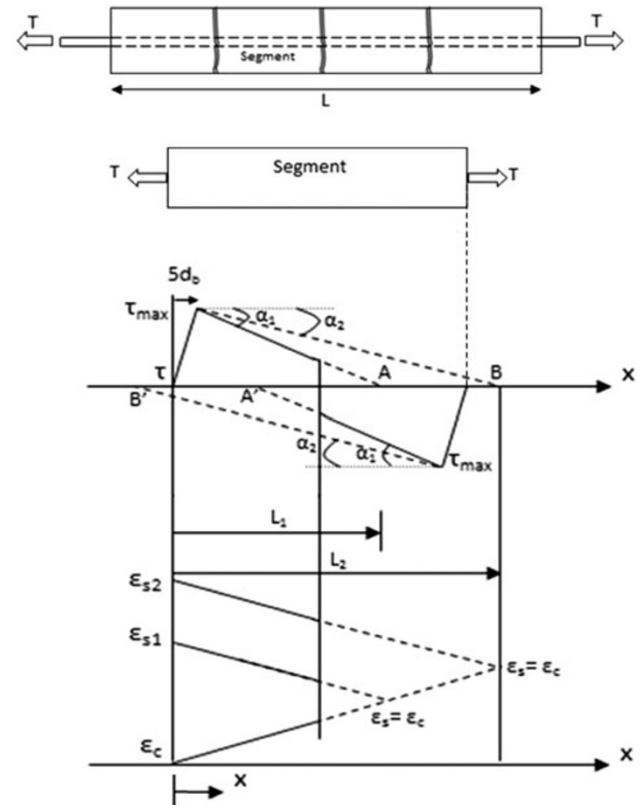


Fig. 3 Bond stress and resulting steel and concrete strain distribution between adjacent cracks in a reinforced concrete member.

tension embedded in a concrete prism; #4 (12.7 mm), #6 (19 mm), #8 (25.4 mm) and #10 (32 mm) bars were considered. The length of the prism, $L = 5,080$ mm (200 in.), is taken to be sufficiently long such that multiple cracks will develop over its length. CEB-FIP Code (1978) reported that the maximum region of concrete affected by a bar in tension is approximately a square area centered on the bar having a dimension $15d_b$. Thus, the minimum tension reinforcing ratio is $\rho_{\min} = (\pi d_b/4)/(15d_b)^2 = 0.0035$ —a value reflected in both the AASHTO (2010) and ACI (2011) codes.

The size of the reinforcing bar (d_b) and the reinforcement ratio ($\rho = A_s/A_c$) are both factors which affect crack development and are varied in this study. Figure 4 represents a simple concrete member reinforced with only one bar. The reinforcement ratio is varied from 0.0035 to 0.02 by changing the area of concrete (i.e., $A_c = A_s/\rho$) that may be effectively engaged by the bar. The reinforcing bar stress-strain relationships used in this study are those determined

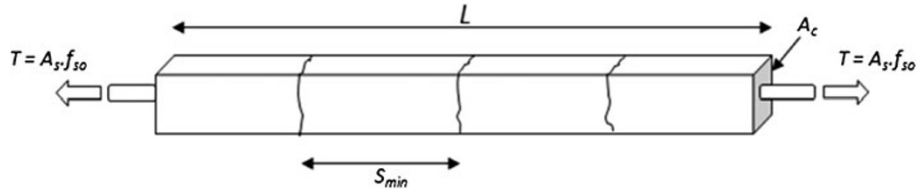


Fig. 4 Direct tension test in the parametric study.

Table 1 Direct tension analysis results (1 MPa = 145.03 Psi; 1 mm = 0.03937 in.).

Bar size material properties	R–O parameters	ρ	Initial crack series		Second crack series		Third crack series	
			f_s (MPa)	s (mm)	f_s (MPa)	s (mm)	f_s (MPa)	s (mm)
#4 $f_u = 1,200$ MPa $f_y = 965$ MPa	$A = 0.004$ $B = 1,186$ $C = 2.8$	0.02	207	159	227	79	nac	
		0.015	262	159	289	79	nac	
		0.01	386	318	469	159	nac	
		0.0075	503	318	613	159	nac	
		0.005	737	635	923	318	nac	
		0.0035	1,034	635	nac			
#6 $f_u = 1,110$ MPa $f_y = 841$ MPa	$A = 0.0203$ $B = 1,365$ $C = 2.4$	0.02	207	159	nac			
		0.015	262	318	310	159	nac	
		0.01	386	318	441	159	nac	
		0.0075	503	635	620	318	nac	
		0.005	730	635	910	318	nac	
		0.0035	1,027	1,270	nac			
#8 $f_u = 1,069$ MPa $f_y = 820$ MPa	$A = 0.0554$ $B = 1,550$ $C = 2.9$	0.02	207	318	227	159	nac	
		0.015	262	318	289	159	nac	
		0.01	379	635	462	318	nac	
		0.0075	496	635	613	318	nac	
		0.005	730	1,270	916	635	nac	
		0.0035	1,027	1,270	nac			
#10 $f_u = 1,069$ MPa $f_y = 820$ MPa	$A = 0.0554$ $B = 1,551$ $C = 2.9$	0.02	207	318	227	159	nac	
		0.015	262	318	289	159	nac	
		0.01	379	635	462	318	nac	
		0.0075	496	635	565	635	586	318
		0.005	730	1,270	923	635	nac	
		0.0035	1,027	2,540	nac			

f_y is the 0.2 % offset strain (ASTM 1035), f_s is the stress level at the crack appearance and s is the crack spacing.

nac no additional cracks.

experimentally (Shahrooz et al. 2011) and represented numerically by a Ramberg–Osgood (R–O) function:

$$f_s = E \varepsilon_s \left\{ A + \frac{1 - A}{[1 + (B \varepsilon_s)^C]^{1/C}} \right\} \leq f_u \quad (11)$$

The experimentally calibrated R–O parameters A , B , and C are given in Table 1. Since no #10 bars were tested, the R–O parameters for #8 (25.4 mm) bars were also applied

to the #10 (32 mm) bars. Although the R–O relationships for high strength steel are used, these are also valid for conventional reinforcing bars through yield since the modulus (E_s) in the R–O relationships is constant to values of stress of about 480 MPa (70 ksi). Thus, the reported data for stress levels below $f_s = 414$ MPa (60 ksi) are valid for both conventional (A615) and high strength (A1035) reinforcing bars. To consider conventional 414 MPa steel in this exercise, simply truncate all data where f_s exceeds 414 MPa.

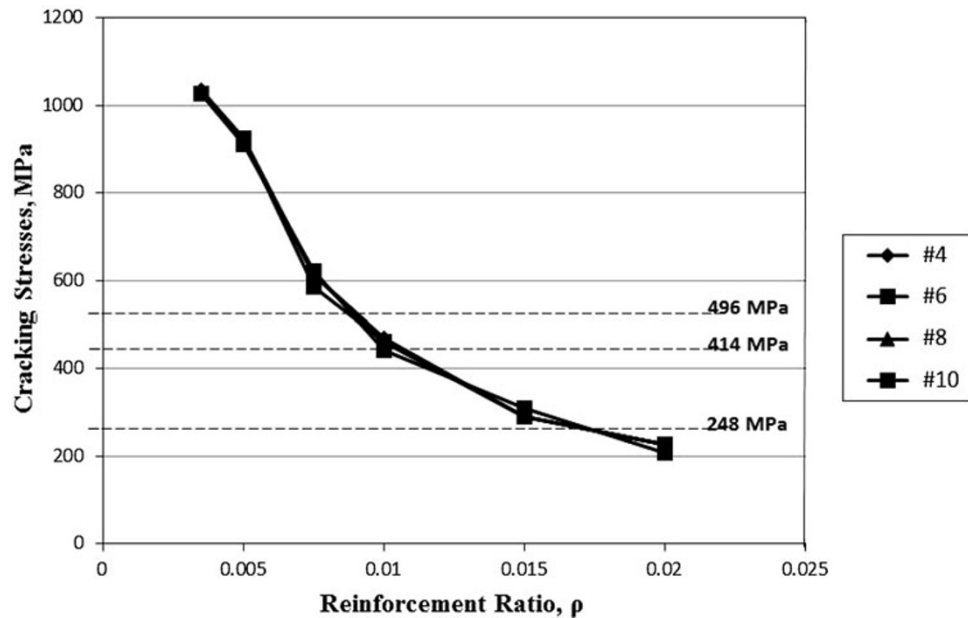


Fig. 5 Corresponding bar stresses causing the last crack formation (based on Table 1) (1 MPa = 145.03 Psi).

The results from this study are shown in Table 1. The concrete assumed to have a compression strength, $f'_c = 34.5$ Mpa. In every case, a 5,080 mm (200 in.) long square concrete prism (Fig. 4) having an area $A_c = A_s/\rho$ is considered. An external tension load is applied to the reinforcing bar up to the bar's ultimate capacity. In Table 1, the values of bar stress, f_s , at which the initial cracks develop, and their spacing (s) are shown. As described above, depending on the value of L_1 subsequent cracking may also develop between these cracks (second and third series). Based on the geometry of the specimen and bar size, there is a specific tension load at which the last series of cracks forms. Further increase of the tension load beyond this load does not result in formation of additional cracks, but only an increase of the existing crack widths. Bar stresses at this final stable crack pattern are established are shown in Fig. 5. Also superimposed on this figure are expected service load stress levels 248, 414, and 496 MPa (36, 60, and 72 ksi), corresponding to $0.60f_y$ for 414, 690, and 827 MPa (60, 100, and 120 ksi) reinforcing steel, respectively. As shown in this figure, the results for different bar sizes are the same and only depend on the reinforcement ratio. Based on the approach taken, all cracks will develop at the same stress and have the same spacing; these values may be considered average values for the concrete and steel considered. Relationships between average and maximum values are discussed briefly below.

Crack development and spacing are affected by bar size and the effective concrete area surrounding the reinforcement. As the reinforcing ratio falls, the behavior becomes dominated by a small number of large cracks (Table 1). Whereas at typical flexural reinforcing ratios (0.01 and 0.015), cracking is better distributed. As the reinforcing ratio becomes larger, cracking remains distributed but crack widths may be expected to be more uniform since cracking stresses vary very little. In all cases, for reinforcing ratio $\rho = 0.01$ and higher, all cracks form at bar stresses below

482 MPa (70 ksi). Consequently, in a concrete section having a reinforcing ratio $\rho = 0.01$ or higher, regardless of steel grade, the crack width and crack spacing are the same. Using higher strength bars allow higher stresses to develop in the steel, but additional cracks are only likely to form at lower reinforcing ratios.

Average crack widths resulting from this analysis, w_{avg} , can be derived from the slip-strain relationship (Eq. 4) as follows:

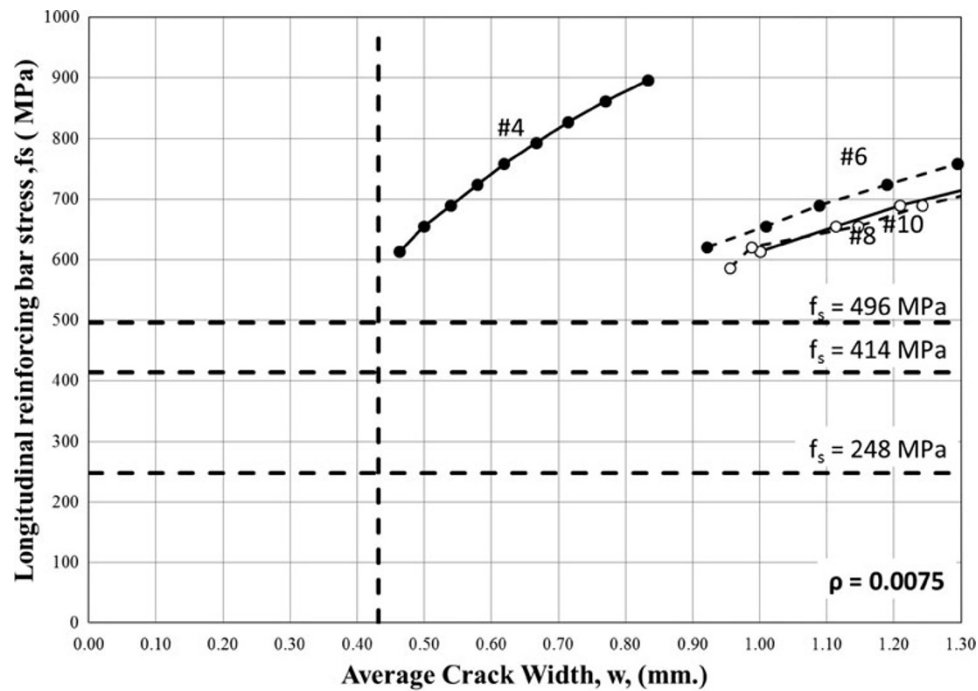
$$w_{avg} = 2 \int_0^{s/2} (\epsilon_s - \epsilon_c) dx \quad (12)$$

The values obtained from this method represent the average crack width along the entire 5,080 mm (200 in.) specimen length. Figure 6 illustrates the average crack widths calculated for the range of reinforcing ratios and bar sizes considered. Figure 6 clearly shows the stress at which the cracks are expected to form (lower left data point in each curve) and the progression of crack opening as the bar stress increases. Also superimposed on this figure are expected service load stress levels 248, 414, and 496 MPa (36, 60, and 72 ksi), corresponding to $0.60f_y$ for 414, 690 and 827 MPa (60, 100, and 120 ksi) reinforcing steel, respectively.

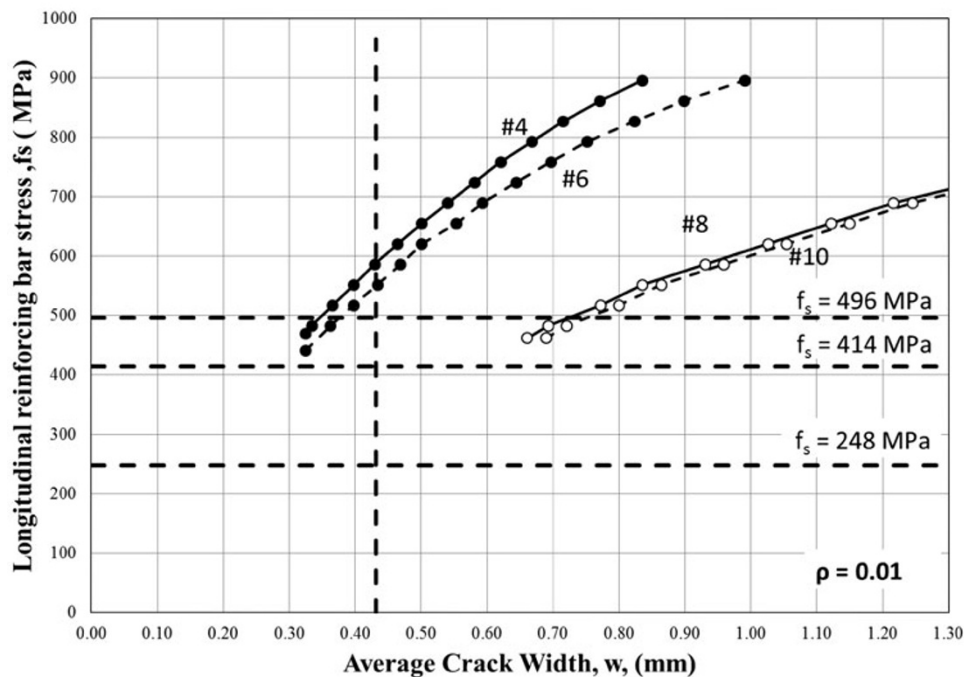
Based on Fig. 6 for $\rho \leq 0.02$, it can be concluded that through reinforcing bar stresses of 496 MPa, average crack widths (it is only possible to consider average crack widths in an analytical context) remain below 0.43 mm (0.017 in.) for all but the largest bars considered (#10). The results were relatively insensitive to changes in reinforcing ratio.

4.2 Experimentally Observed Crack Widths

The parametric study of crack opening in a prism under direct tension is a simplified approach in calculating the crack widths in concrete beams. The obtained result from



Predicted crack widths from parametric study. $\rho = 0.0075$



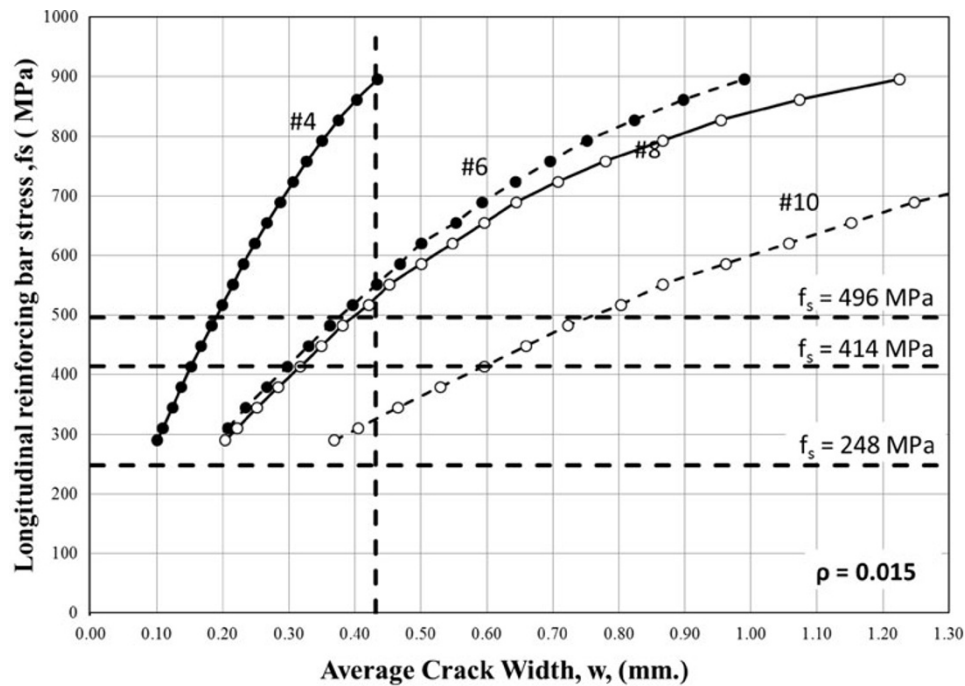
Predicted crack widths from parametric study. $\rho = 0.01$

Fig. 6 The extension of crack opening versus reinforcing bar stresses (1 MPa = 145.03 Psi; 1 mm = 0.03937 in.).

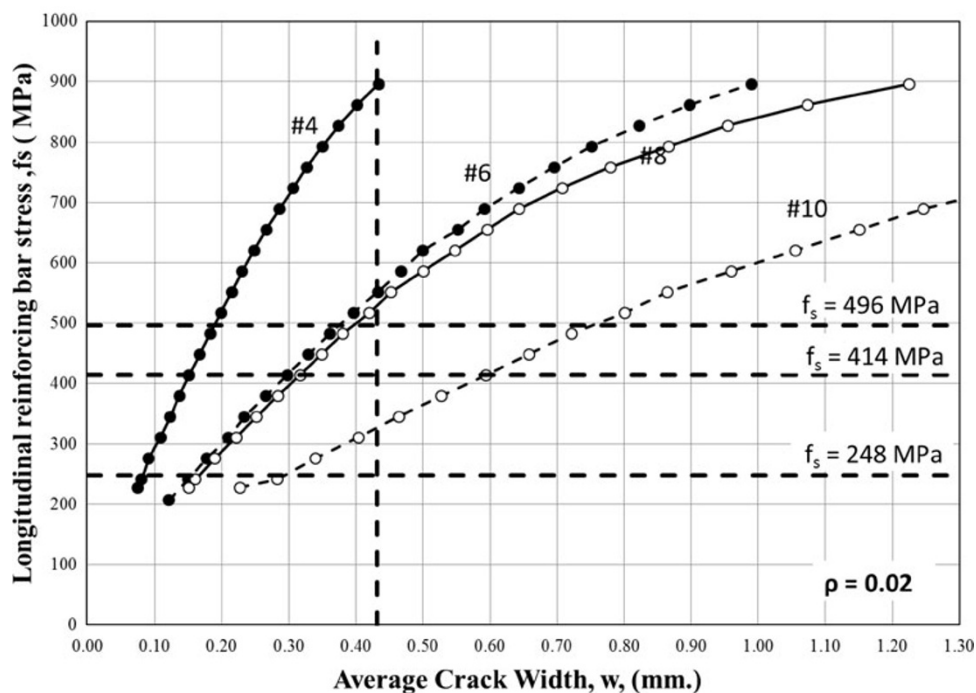
parametric study should be confirmed by comparing to some experimental data. Therefore, extensive crack width data were collected from flexural test specimens F1 to F6 tested as part of the NCHRP 12-77 study (Shahrooz et al. 2011). A summary of these specimens is shown in Table 2. To assess the effects of using higher strength steel, the measured crack widths corresponding to various stresses in the reinforcing steel are plotted in Fig. 7.

Figure 7a provides the average crack widths measured from all cracks in the 1,016 mm (40 in.) long constant

moment region (see Table 2). Figure 7b provides the maximum crack width measured in this region. The ratio of maximum to average measured crack widths for all specimens at all stress levels is 1.8, consistent with available guidance for this ratio, which tends to range between 1.5 and 2.0 (Chowdhury and Loo 2001). In all cases, the ratio of maximum to average crack width falls with increasing bar stress. At approximately 248 MPa (36 ksi), this ratio is 1.7, falling to 1.6 at 414 MPa (60 ksi), and 1.5 at 496 MPa (72 ksi).



Predicted crack widths from parametric study. $\rho = 0.015$



Predicted crack widths from parametric study. $\rho = 0.02$

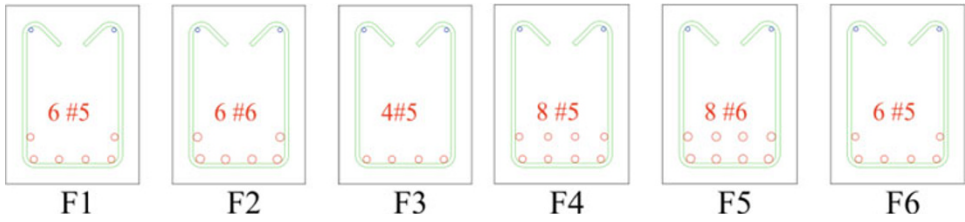
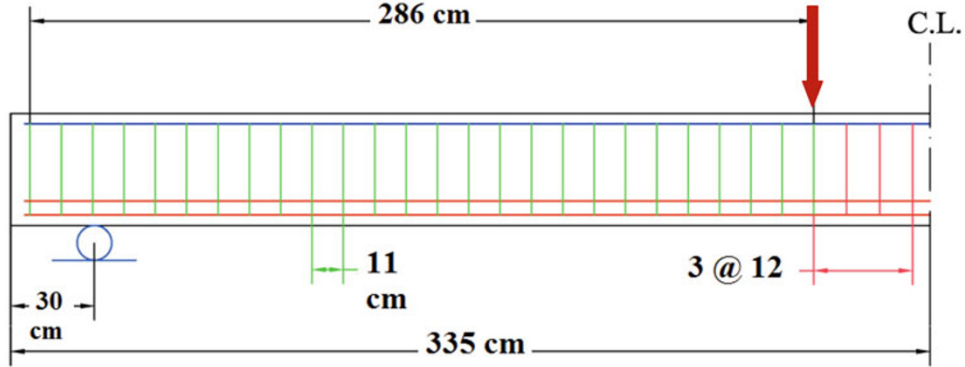
Fig. 6 continued

The data shown in Fig. 7 clearly show that at rational service load levels ($f_s < 496$ MPa 72 ksi), average crack widths are all below the present AASHTO de facto limit of 0.43 mm (0.017 in.). Indeed, with the exception of beam F2, maximum crack widths also fall below this threshold through bar stresses of 496 MPa (72 ksi). Crack width is largely unaffected by the reinforcing ratio within the range considered. It is noted that all 305 mm (12 in.) wide beams had four bars [#5 (15.9 mm) or #6

(19 mm)] in the lowermost layer; thus, crack control reinforcing would be considered excellent for these beams.

Considering the measured crack widths in this experimental study, it appears that the existing equations are inherently conservative. This conservativeness allows present specifications to be extended to the anticipated higher service level stresses associated with the use of high strength reinforcing steel.

Table 2 Details of flexural beam specimens F1–F6 (Shahrooz et al. 2011).

	F1	F2	F3	F4	F5	F6
A1035 longitudinal steel						
Lower layer	4 #5	4 #6	4 #5	4 #5	4 #6	4 #5
Second layer	2 #5	2 #6	n.a.	4 #5	4 #6	2 #5
$\rho = A_s/bd$	0.012	0.016	0.007	0.016	0.023	0.012
f_y (0.2 % offset) (MPa)	897	839	897	890	926	890
R–O parameters						
A	0.0145	0.0203	0.0145	0.0145	0.0130	0.0145
B	1,282	1,282	1,282	1,282	1,282	1,282
C	2.5	2.4	2.5	2.5	2.5	2.5
f'_c (MPa)	89	89	89	114	112	116
Specimen cross sections						
Specimen elevation						

1 MPa = 145.03 psi; 1 cm = 0.3937 in.

5. Conclusions

Based on the results of flexural tests conducted as part of a related study, crack widths at service load levels were evaluated and found to be within presently accepted limits, and were predictable using current ACI (2011) or AASHTO (2010) provisions. A limitation on service-level stresses of $f_s \leq 414$ MPa (60 ksi) is recommended; this is consistent with a related recommendation that $f_y \leq 689$ MPa (100 Ksi) (Shahrooz et al. 2011).

Based on a parametric study on crack widths, it is shown that crack development and spacing are affected by bar size

and the effective concrete area surrounding the reinforcement. As the reinforcing ratio falls, the behavior becomes dominated by a small number of large cracks. Whereas for typical reinforcing ratios (0.01 and 0.015), cracking occurs in a more progressive manner and is better distributed, and hence some variation in crack width along the member should be expected. As the reinforcing ratio becomes larger, cracking remains distributed but crack widths may be expected to be more uniform since cracking stresses vary very little. In all cases considered, for reinforcing ratios $\rho = 0.01$ and higher, cracks form at bar stresses below 482 MPa (70 ksi). Consequently, in a concrete section with

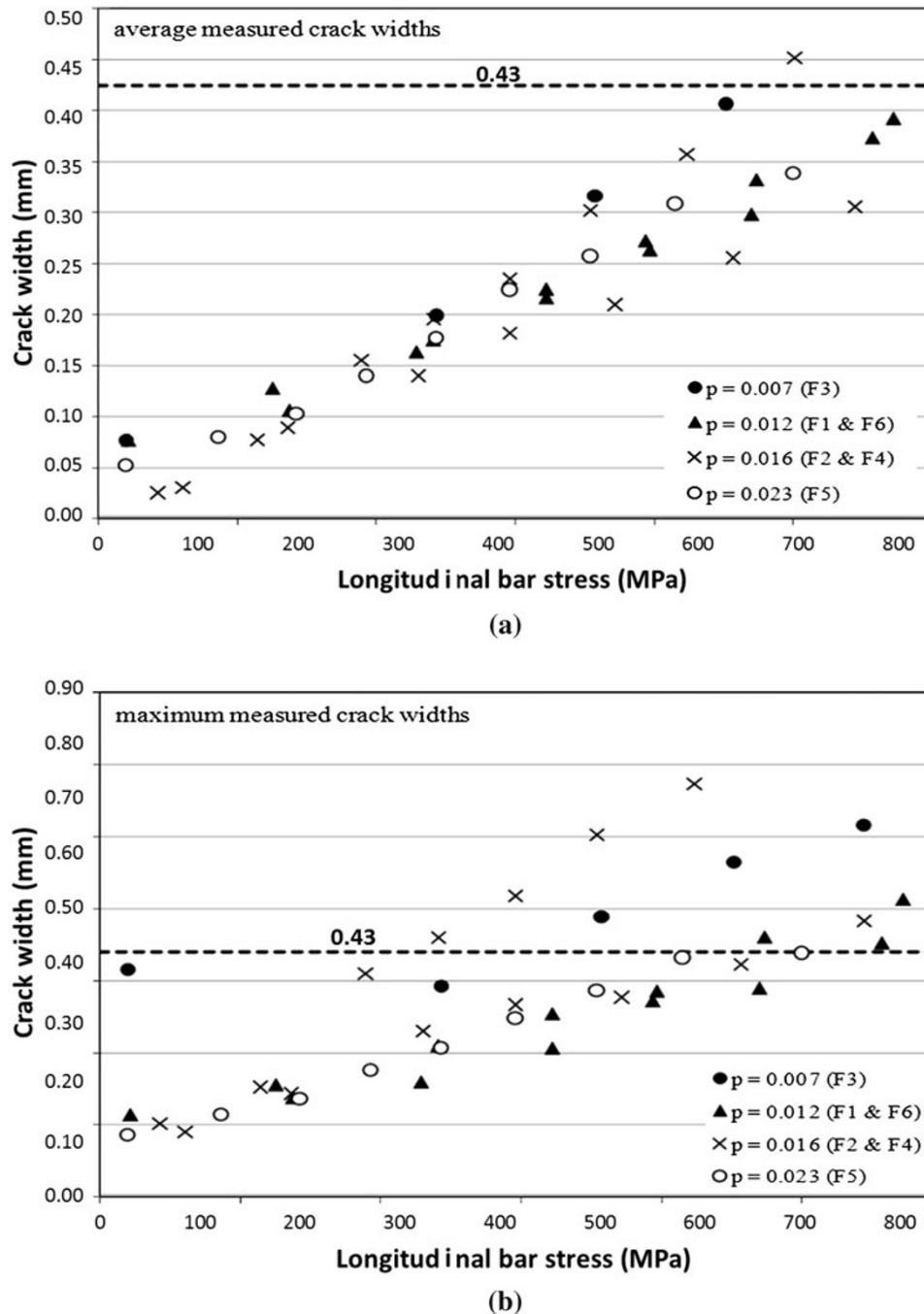


Fig. 7 Measured crack widths with longitudinal reinforcing bar stress for flexural beams (1 MPa = 145 psi; 1 mm = 0.03937 in.).
a Average crack widths. **b** Maximum crack widths.

reinforcing ratio $\rho = 0.01$ or higher, regardless of reinforcing grade, the crack width and crack spacing will be similar.

Based on this study, it can be concluded that through reinforcing bar stresses of 496 MPa (72 ksi), average crack widths remain below 0.43 mm (0.017 in.) for cases having $\rho < 0.02$ and for all but the largest bars considered [#10 (32 mm)]. The results were relatively insensitive to changes in reinforcing ratio. These results were confirmed by comparison to available experimental data. The ratio of maximum to average crack width was observed to be slightly less than that commonly associated with conventional 414 MPa (60 ksi) reinforcing steel. Additionally, this ratio decreased at higher stress levels.

Open Access

This article is distributed under the terms of the Creative Commons Attribution License which permits any use, distribution, and reproduction in any medium, provided the original author(s) and the source are credited.

References

- AASHTO. (2010). *AASHTO LRFD bridge design specifications* (5th ed.). Washington, DC: American Association of State Highway and Transportation Officials.

- ACI Committee 318. (2011). *ACI 318-11 building code requirements for reinforced concrete and commentary*. Farmington Hills, MI: American Concrete Institute.
- Bischoff, P. H. (2005). Reevaluation of deflection prediction for concrete beams reinforced with steel and fiber reinforced polymer bars. *Journal of Structural Engineering, ASCE*, 131(5), 752–767.
- Bischoff, P. H. (2007). Rational model for calculating deflection of reinforced concrete beams and slabs. *Canadian Journal of Civil Engineering*, 34, 992–1002.
- Bischoff, P. H., & Paixao, R. (2004). Tension stiffening and cracking of concrete reinforced with glass fiber reinforced polymer (GFRP) bars. *Canadian Journal of Civil Engineering*, 31, 579–588.
- Broms, B. B. (1965a). Technique for investigation of internal cracks in reinforced concrete members. In *ACI Journal, Proceedings* (Vol. 62, No. 1, pp. 35–44). Jan. 1965.
- Broms, B. B. (1965b). Crack width and crack spacing in reinforced concrete members. In *ACI Journal, Proceedings* (Vol. 62, No. 10, pp. 1237–1256), Oct. 1965.
- CEB-FIP Model Code. (1990). In *Comite Euro-International du Beton*, June 1991.
- CEB-FIP, Model Code for Concrete Structures. (1978). *CEB-FIP international recommendations* (3rd ed., p. 348). Paris, France: Comite Euro-International du Beton.
- Chowdhury, S. H., & Loo, Y. C. (2001). A new formula for prediction of crack widths in reinforced and partially prestressed concrete beam. *Advances in Structural Engineering*, 4(2), 101–109.
- Frosch, R. J. (1999). Another look at cracking and crack control in reinforced concrete. *ACI Structural Journal*, 96(3), 437–442.
- Frosch, R. J. (2001). *Flexural crack control in reinforced concrete, design and construction practices to mitigate cracking SP 204* (pp. 135–154). Farmington Hills, MI: American Concrete Institute.
- Kwak, H. G. & Filippou F. C. (1990), *Finite element analysis of reinforced concrete structures under monotonic loads*, A report No. UCB/SEMM-90/14. University of California, Berkeley, CA.
- Nawy, E. G. (1968). Crack control in reinforced concrete structures. In *Journal of the American Concrete Institute, Proc.* (Vol. 65, pp. 825–838). Farmington Hills, MI, October 1968.
- Ng, P. L., Lam, J. Y. K., & Kwan, A. K. H. (2010). Tension stiffening in concrete beams. Part 1: FE analysis. *Proceedings of the ICE—Structures and Buildings*, 163(1), 19–28.
- Odman, S. T. A. (1962). *Stresses in axially reinforced concrete prisms subjected to tension and exposed to drying*. Stockholm: Swedish Cement and Concrete Research Institute at the Royal Institute of Technology, NR34.
- Reis, E. E. Jr., Mozer, J. D., Bianchini, A. C. and Kesler, C. E. (1964). *Causes and control of cracking in concrete reinforced with high strength steel Bars—A review of research*, T. & A. M. Report No. 261, University of Illinois, IL.
- Shahrooz, B. M., Miller, R. A., Harries, K. A. & Russell, H. G. (2011). *Design of Concrete Structures Using High-Strength Steel Reinforcement*, NCHRP Report 679, Transportation Research Board, 83 pp + appendices.
- Thomas, F. G. (1936). Cracking in reinforced concrete. *The Structural Engineer*, 14, 298–320.